On the morphological characteristics of overdeepenings in high-mountain glacier beds

Wilfried Haeberli[1], Andreas Linsbauer[1,2], Alejo Cochachin[3], Cesar Salazar[3], Urs H. Fischer[4]

1. Geography Department, University of Zurich, Zurich, Switzerland
2. Department of Geosciences, University of Fribourg, Fribourg, Switzerland
3. Glaciology and Water Resources Unit, Huaraz, Peru
4. National Cooperative for the Disposal of Radioactive Waste, Nagra, Wettingen, Switzerland

email of corresponding author: wilfried.haeberli@geo.uzh.ch

Supplementary material

S1 Glacier-bed overdeepenings and safety aspects

Within the framework of analyses concerning the long-term safety of repositories for radioactive waste, conditions during possible future glacials are systematically investigated. Such glacial conditions can affect subsurface repositories through the stresses imposed by large foreland glaciers, the penetration of peri- and subglacial permafrost to greater depth, the influence of both glaciers and permafrost, in sometimes complex interaction, on groundwater hydraulics and flow, but especially also through efficient deep erosion by glaciers and their basal melt-water discharge (Fischer et al., 2014). Interest thereby focuses on glacial overdeepenings, closed topographic depressions in former or existing glacier beds, which are characteristic for glacially sculpted landscapes (Cook and Swift, 2012). The present study concerning glacial overdeepenings in high-mountain regions was carried out within

the framework of studies about possible effects from future glacial conditions on radioactive waste repositories in Switzerland (cf. the international workshop reports by Fischer and Haeberli, 2010, 2012). It is parallel and complementary to the study by Patton et al. (2015) about controls on the location and evolution of subglacial overdeepenings below ice sheets and to the work of Werder (2016) on adverse slopes and overdeepening depths. Its results are also of interest in connection with safety considerations (hazards from impact waves, overtopping, dam breaching, floods, debris flows; cf. Haeberli et al., 2016) or the potential use for hydropower production, water supply and tourism of lakes newly forming in cold mountain chains as a consequence of continued atmospheric warming and deglaciation. It therefore also relates to work about new lakes in the Swiss Alps performed by the recently completed NELAK-project (NELAK 2013; cf. also Haeberli and Linsbauer, 2013), to the modelling of glacier-bed topographies and potential new lakes in the Himalaya-Karakoram region (Frey et al., 2014; Linsbauer et al., 2016) and to long-term work about hazardous glacier lakes in Peru (Portocarrero, 2013).

S2 Glacier ice-thickness distribution, modelled bed topography and detected overdeepenings

In combination with high-resolution digital terrain information, slope-related approaches for ice thickness estimation at glaciers enable the calculation of quite detailed glacier-bed topographies (Farinotti et al., 2009; Linsbauer et al., 2009, 2012; Huss and Farinotti, 2012; Clarke et al., 2013; Frey et al., 2014). Slope-related modelling of ice-thicknesses and glacier-bed topographies are based on the principle of an inverse flow law of ice, where mass turn-over as determined by climatic and topographic conditions governs strain rates and corresponding basal shear stresses. Basal shear stress then couples surface slope with ice thickness. Absolute values of ice-depth estimations thereby remain rather uncertain (on average around ± 30% of the estimated value as directly compared to local point or profile measurements from drilling, radio-echo sounding, etc.; Linsbauer et al., 2012). This is primarily due to still imprecisely understood aspects related to the quantification of mass fluxes and flow for glaciers with unknown bed topography (surface mass balance, basal sliding, etc.; Haeberli, 2016). In contrast, relative differences within individual glaciers reflecting

spatial patterns of ice thickness and corresponding bed topographies are primarily related to surface slope as given by DEMs and, hence, are much more robust (cf. the model inter-comparison in figure 6 of Frey et al. 2014). The main uncertainty concerning bed topographies relates to the filtering/smoothing, which is necessary to account for effects of longitudinal stress coupling in glaciers. This uncertainty about longitudinal smoothing is especially important concerning modelled bed overdeepenings (Adhikari and Marshall, 2013) and needs further investigation.

Three primary approaches presently exist:

(1) *Stress-driven models* (Linsbauer et al. 2009, 2012; Paul and Linsbauer 2012; Frey et al., 2014) assume a constant shear stress for each individual glacier as defined by an empirical relation between average basal shear stress and glacier elevation range governing mass turn-over (Haeberli and Hoelzle, 1995). This approach is simple and empirical but has the advantage of only requiring easily available input information and of being transparent, robust and fast in its application.

(2) *Flux-driven models* (Farinotti et al., 2009, Huss and Farinotti, 2012) parameterize a complex set of processes to simulate surface mass flux and corresponding flow of ice; basal shear stresses are not assumed a priori but produced by such models and can vary within individual glaciers. This elegant approach involves a comprehensive process understanding. Many of the involved processes can, however, not precisely be parameterized (see explanation above). Heavy tuning is therefore necessary, which reduces the pursued complexity and makes the approach quite empirical again.

(3) *Combined flux/stress-driven models* (Clarke et al., 2013) combine the approaches (1) and (2). They optimize the use of all available information (mass flux, shear stress) but leave reduced possibilities for independent comparison with the approaches (1) and (2).

All calculations in this paper were made with the stress-driven models GlabTop and GlabTop2. An inter-comparison made by Frey et al. (2014; especially their Figure 9) shows that average basal shear stresses calculated using the flux-driven approach of Huss and Farinotti (2012) are in satisfactory agreement with the shear stress range used by the GlabTop2 model for elevation ranges up to 3000 m, which are characteristic for the Alps. The calculated average thickness values differ within a

small range, which is even comparable with the uncertainty of results from depth determinations by drilling and/or geophysical soundings in the field. This is hardly astonishing as the involved models are tuned, calibrated or validated with similar information from field measurements. One main difference is the smoothing, which is applied over 200 m elevation belts in the worldwide calculation by Huss and Farinotti (2012) but over 50 m elevation belts for GlabTop and GlabTop2. Thereby the smoothing corresponds to a slope averaging over a reference distance of 5-10 times the local ice thickness, which is considered to be realistic and practicable even for small glaciers.

The resulting ice thickness distribution is subtracted from the surface DEM to obtain the bed topography, i.e., a DEM without glaciers. The overdeepenings in the glacier beds are detected by filling them with a standard geoinformatic hydrology tool (ESRI 2011) and a slope grid derived from the filled DEM. By selecting slope values smaller than one degree within the glacier outlines, the overdeepenings in the glacier beds are found. The difference grid between the filled DEM and the former DEM without glaciers is used to quantify the area and volume of the overdeepenings. The mean and maximum depths of the potential lakes are also calculated with zonal statistics (Linsbauer et al., 2012, 2016).

S3 Extraction of parameters from modelled overdeepenings

Parameters of interest

General process understanding of glacier flow and erosion (Fischer and Haeberli, 2010, 2012), rather sparse field measurements (boreholes, geophysics) and observations on recently exposed glacier beds (bathymetries) indicate that low ice surface slopes (< 5 to 10°), compressive ice flow, high basal water pressure (low effective normal pressure), damped water pressure fluctuations and slow subglacial water flow velocities are characteristic of overdeepened parts of glacier beds. In contrast, increasing ice surface slopes, lateral flow constriction, ice thickness reduction, extending flow (causing crevassing opening) and increasing drainage efficiency (increasing water flow velocities and decreasing water pressures) are characteristic for the bedrock thresholds (known as riegels) at the lower end of overdeepened areas. Bed overdeepening tends to occur where ice is (or has been)

warm-based, which enables sliding and thus erosion, and where surface water is produced and is able to reach the bed, as this promotes rapid sliding, stimulates quarrying, and enables efficient sediment flushing, thereby preventing the accumulation of thick till layers that would prevent deep bedrock erosion. Basal shear stress and ice thickness can vary within wide ranges.

Modelling with GlabTop produces not only ice thickness distributions, bed topographies and the outlines of potential overdeepenings, but also further datasets which can be used for extracting parameters to describe the morphological characteristics of bed overdeepenings, i.e. derivatives (like slopes) from the different DEMs (Input DEM, DEM without glaciers, filled DEM), a bathymetry raster file of the overdeepenings and various attribute tables with statistical values for glaciers and overdeepenings. Of primary interest for a statistical analysis of the morphological characteristics of overdeepenings are the following parameters (here given with their operationalization):

Numerical parameters

1. Area of the overdeepenings (from the polygon delineating it).
2. Maximum and mean depth (derived with zonal statistics on the bathymetry grid, taking the polygons of the overdeepenings as zones).
3. Volume (calculated from area and mean depth of the overdeepening).
4. Length (longest line and orientation) within the boundaries of the overdeepening (defined as the longest line completely embedded within a polygon).
5. Maximum width (perpendicular to the longest line) and mean width (total area divided by the maximum length = longest line).
6. Elongation (width-to-length ratio to obtain convenient numbers between 0 and 1).
7. Length with respect to the flow direction (length and orientation; straight-line distance between the inlet and outlet according to the flow routing based on the bed topography DEM).
8. Maximum and mean inclination of adverse and normal slopes (along the line connecting the point of maximum depth with the outlet/inlet points).

9. Average basal shear stress of the glaciers (from glacier elevation range following Haeberli and Hoelzle 1995; this value is a basic model assumption and taken to be constant within each individual glacier).

Expert judgments

10. Basal ice temperature (temperate or cold; estimated for each individual glacier by expert judgement (cf. Haeberli and Hoelzle, 1995, Ryser et al., 2013, Suter et al., 2001).
11. Topological classification of overdeepenings with respect to glacier flow (estimated by expert judgement using the following scheme; note that the category “diffluence” does not occur in the Alps today and that the category “terminus” is delicate as present-day ice margins are far retreated and may not be typical for times when overdeepenings formed.):
    a. cirque
    b. confluence
    c. diffluence
    d. trunk valley
    e. terminus
    f. unclassified
12. Classification of dam/outlet (estimated by expert judgement based mainly on the erosion/sedimentation index for glaciers and field evidence from exposed glacier forefields (cf. Zemp et al., 2005)).

Semi-automatic GIS tool to extract the parameters

The above-listed parameters were extracted manually from the bathymetries of the Peruvian lakes. A series of tools were developed in a GIS environment to extract the corresponding and operationalized parameters from the modelled overdeepenings. The following explanations demonstrate how the values have been calculated (Figure S3).

Maximum length: The function “geom.polyfetch” from Geospatial Modelling Environment (GME 2013) was used to derive the longest line within a polygon. The length and angle of the line is assigned in the attribute table.

Maximum width: Perpendicular to the lines of maximum length, lines at distances of 50 m are created which reach the outlines of the overdeepening. The longest one is chosen to be the maximum width. This information is stored in the attribute table.

Maximum depth: Based on the DEM without glaciers, the flow direction grid (a raster of flow directions along the steepest gradient from each cell to the steepest downslope neighbour) is calculated, afterwards the sinks in the overdeepenings are extracted and their depth is calculated from the bathymetry grid. The sink point with the highest value in terms of depth is the point within the polygon of the overdeepening with the maximum depth.

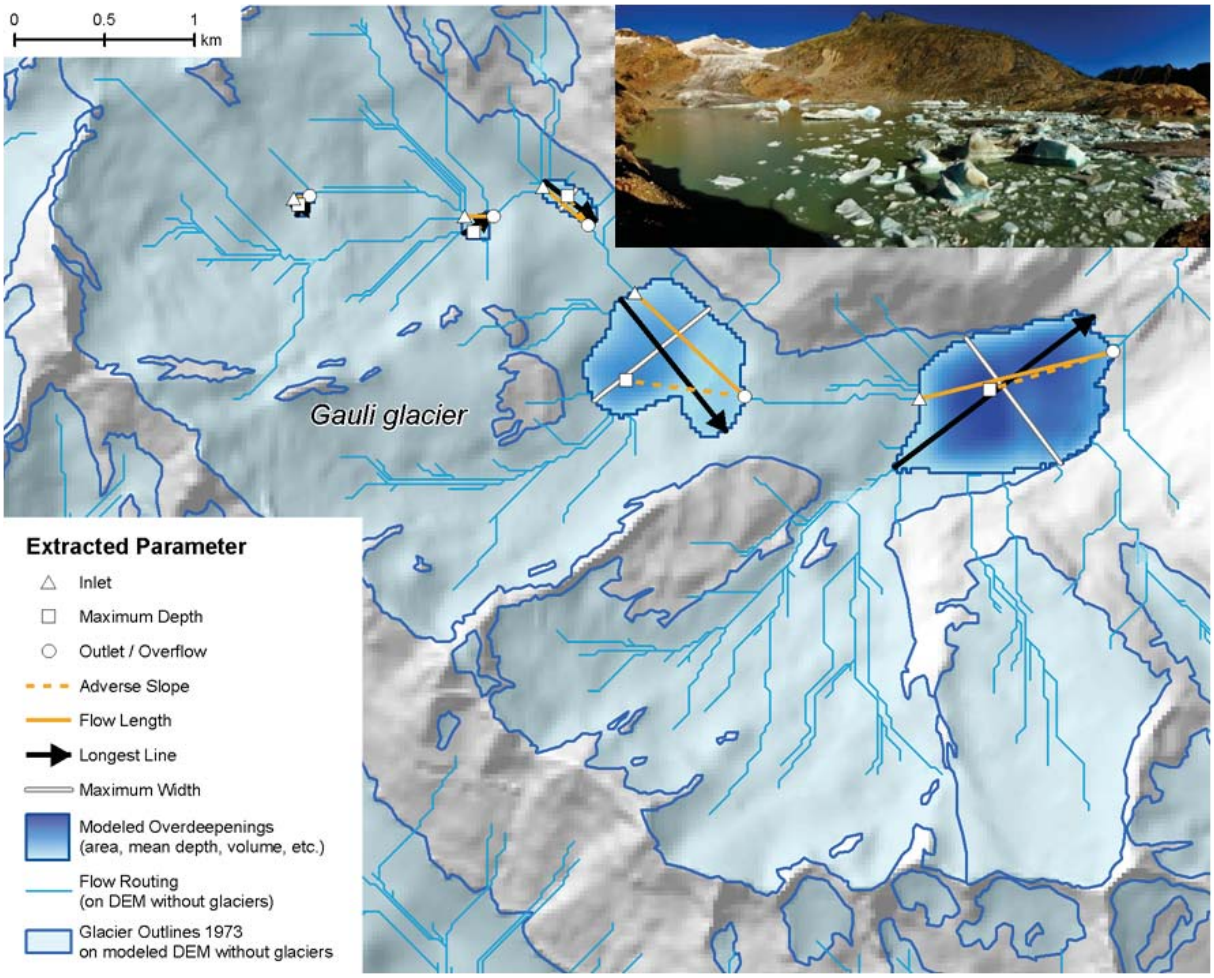

Figure S3: Map depicting the outlines of glaciers in the Gauli region in 1973, draped over the glacier bed modelled with GlabTop. Overdeepenings, flow routing and further parameters shown in the legend are derived from the bed-topography DEM. Photograph on top right shows Gauli glacier with its recently formed lake in the forefield (the picture was taken from the south shore of the lake by Bruno Petroni in August 2009; swisseduc.ch/glaciers).

Flow routing - inlets and outlets: The standard hydrologic toolset in GIS environments to derive streamlines is applied to the filled DEM without glaciers (that includes: Flow Direction, Flow Accumulation, Stream Network, Stream Order, Stream To Feature). The streamlines are intersected with the polygons of the overdeepenings resulting in points along the edge of the overdeepenings, representing all inlets and the outlet of the streamlines of an overdeepening (Figure S3). The outlet is found by choosing the point with the highest Shreve order value (the method of stream ordering by magnitude, proposed by Shreve (1966) - all links with no tributaries are assigned a magnitude (order) of one; magnitudes are additive downslope, when two links intersect, their magnitudes are added and assigned to the downslope link (ESRI, 2014)). The major inlet is found by choosing the intersection point with the lowest intersection order value, the highest Shreve order value and the highest elevation on the surface DEM.

Flow length, adverse and normal slope: The line depicting the length of an overdeepening with respect to the flow direction is found by connecting the inlet and outlet as defined above. For these lines the length and the orientation is extracted. The lines of adverse and normal slopes are found by connecting the point of maximum depth with the outlet and inlet, respectively. Values for maximum and mean adverse and normal slopes are calculated from all the grid cells within a distance of 50 m around the lines derived before. From maximum depth and length also the trigonometric value (ATAN) of the adverse and normal slope can be calculated.

S4 Substrate and dam material

For the glaciers of the Swiss Alps, bed characteristics were estimated based on the erosion/sedimentation-index (Figure 7; Haeberli, 1996; Zemp et al., 2005; Fischer and Haeberli, 2010). This index is a combination of factors affecting the sediment balance of a glacierized mountain catchment, i.e. the ratio between debris input from the surrounding rock walls and debris evacuation by the melt water stream; it distinguishes between glaciers eroding into bedrock and those building up sedimentary beds.

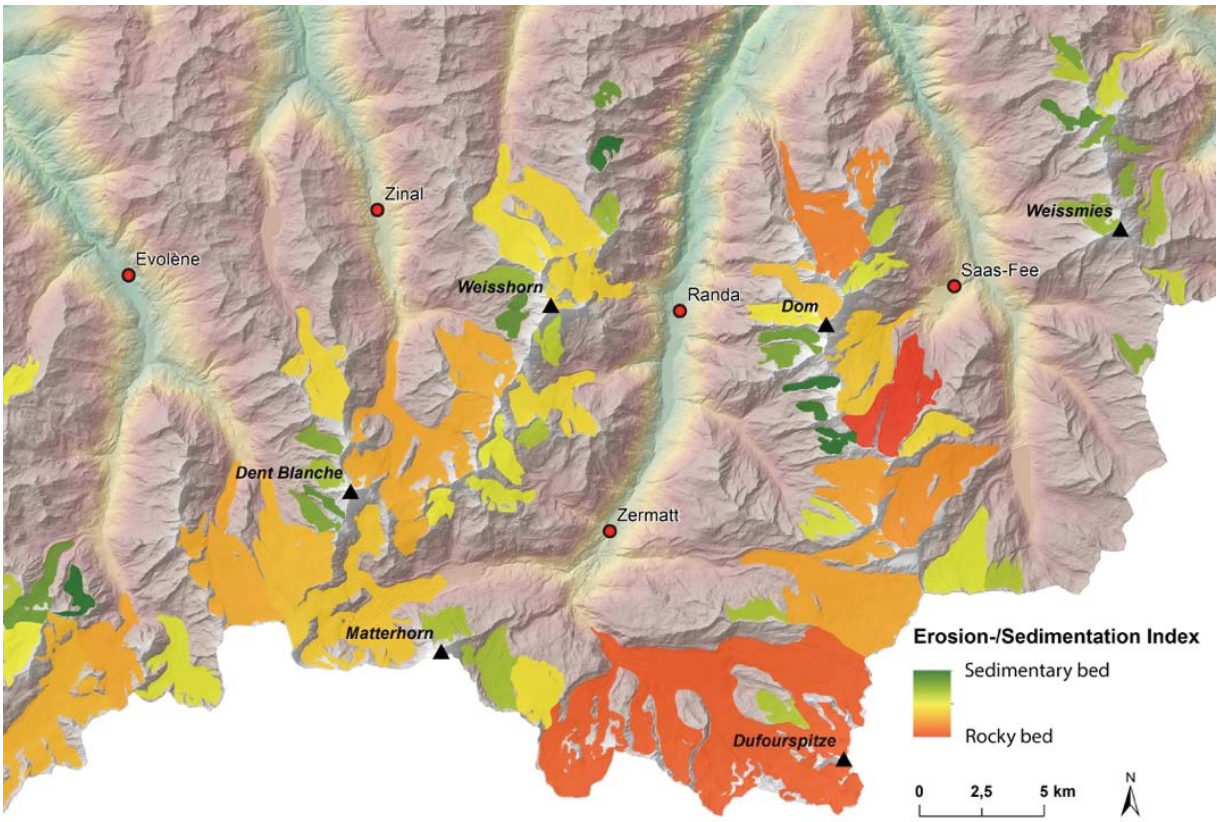

Figure S4: Indexed glacier beds in the Valais Alps, Switzerland, showing five classes going from rocky beds (red) to sedimentary beds (green). Computing and graph by Nico Moelg

S5 Additional scatter plots of morphometric parameters

Additional scatter plots of morphometric parameters are provided in Figure S5.

(a) mean depth as a function of area, length, width and elongation

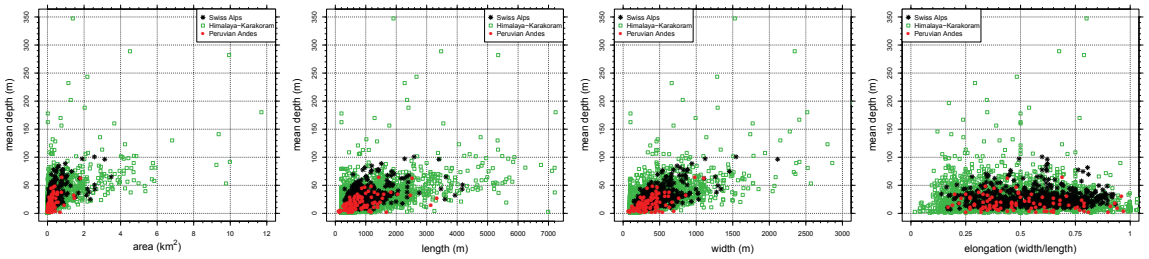

(b) mean adverse slope as a function of area, length, width and elongation

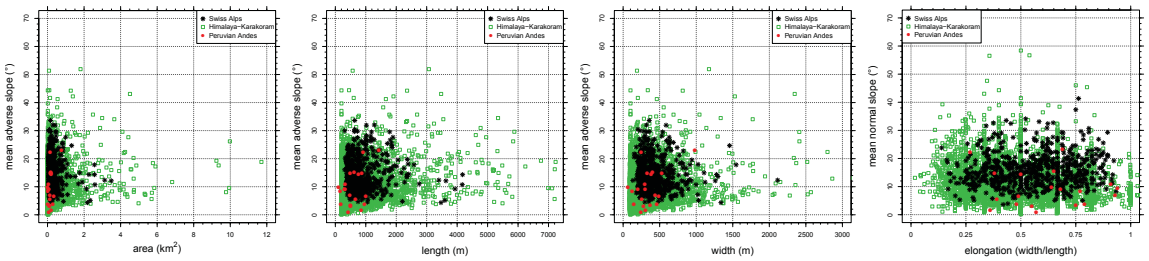

(c) maximum/mean adverse slope vs. maximum/mean normal slope

(d) maximum adverse/normal slope vs. mean adverse/normal slope

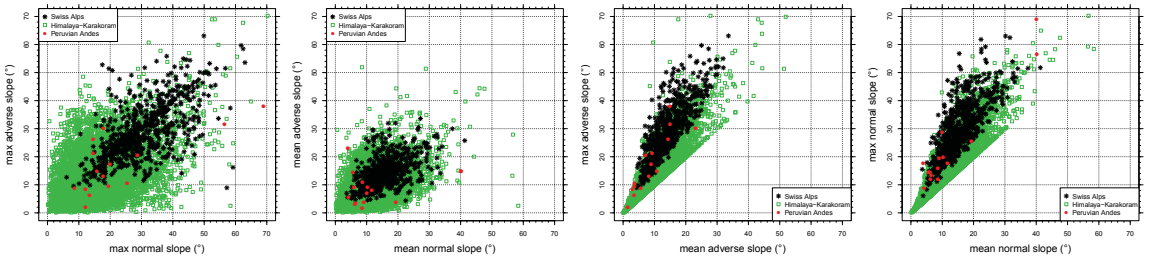

(e) maximum/mean adverse slope vs. mean depth

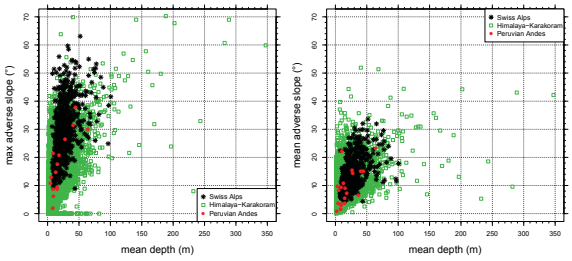

Figure S5: Additional scatter plots of morphometric parameters

REFERENCES

Adhikari S, Marshall SJ. 2013. Influence of high-order mechanics on simulation of glacier response to climate change: insights from Haig Glacier, Canadian Rocky Mountains. The Cryosphere 7(5), 1527–1541, doi:10.5194/tc-7-1527-2013.

Clarke GKC, Anslow SF, Jarosch AH, Radić V, Menounos B, Bolch T, Berthier E. 2013. Ice volume and subglacial topography for western Canadian glaciers from mass balance fields, thinning rates, and a bed stress model. Journal of Climate 26, 4282-4303.

Cook SJ, Swift DA. 2012. Subglacial basins: Their origin and importance in glacial systems and landscapes. Earth Science Reviews 115, 332-372, doi:10.1016/j.earscirev.2012.09.009.

ESRI. 2011. ArcGIS Desktop: Release 10. Environmental Systems Research Institute (ESRI), Redlands, CA

Farinotti D, Huss M, Bauder A, Funk M, Truffer M. 2009. A method to estimate the ice volume and ice-thickness distribution of alpine glaciers. Journal of Glaciology 55, 422-430, doi: 10.3189/002214309788816759.

Fischer UH, Haeberli W. 2010. Glacial erosion modelling – results of a workshop held in Unterägeri, Switzerland, 29 April - 1 May 2010. Nagra Arbeitsbericht NAB 10-34. Wettingen, Switzerland.

Fischer UH, Haeberli W. 2012. Glacial overdeepening – results of a workshop held in Zürich, Switzerland, 20-21 April 2012. Nagra Arbeitsbericht NAB 12-48, Wettingen, Switzerland.

Fischer UH, Bebiolka A, Brandefelt J, Follin S, Hirschorn S, Jensen M, Keller S, Kennel lL, Näslund J-O, Normani S, Selroos J-O, Vidstrand R. 2014. Radioactive waste under conditions of future ice ages. In: Haeberli W, Whiteman C (Eds): Snow and Ice-Related Hazards, Risks and Disasters. Elsevier, Amsterdam, etc., 345-393.

Frey H, Machguth H, Huss M, Huggel C, Bajracharya S, Bolch T, Kulkarni A, Linsbauer A, Salzmann N, Stoffel M. 2014. Estimating the volume of glaciers in the Himalaya-Karakoram region using different methods. The Cryosphere 8, 2313-2333, doi:10.5194/tc-8-2313-2014.

GME. 2013. http://www.spatialecology.com/gme/index.htm (access date: 13.08.2013)

Haeberli W. 1996. On the morphodynamics of ice/debris-transport systems in cold mountain areas. Norsk Geografisk Tidsskrift 50, 3-9.

Haeberli W. 2016. On area- and slope-related thickness estimates and volume calculations for unmeasured glaciers. The Cryosphere Discussion, doi:10.5194/tc-2015-222.

Haeberli W, Hoelzle M. 1995. Application of inventory data for estimating characteristics of and regional climate-change effects on mountain glaciers: a pilot study with the European Alps. Annals of Glaciology 21, 206-212. Russian Translation in: Data of Glaciological Studies, Moscow, 82, 116-124.

Haeberli W, Linsbauer A. 2013. Global glacier volumes and sea level – small but systematic effects of ice below the surface of the ocean and of new local lakes on land. Brief communication, The Cryosphere 7, 817-821, doi:10.5194/tc-7-817-2013.

Haeberli W, Schaub Y, Huggel C. 2016. Increasing risks related to landslides from degrading permafrost into new lakes in de-glaciating mountain ranges. Geomorphology, doi:10.1016/j.geomorph.2016.02.009.

Huss M, Farinotti D. 2012. Distributed ice thickness and volume of all glaciers around the globe. Journal of Geophysical Research 117 (F4), F04010, doi: 10.1029/2012JF002523.

Linsbauer A, Paul F, Hoelzle M, Frey H, Haeberli W. 2009. The Swiss Alps without glaciers – a GIS-based modelling approach for reconstruction of glacier beds. Proceedings of Geomorphometry 2009, Zurich, Switzerland, 243-247.

Linsbauer A, Paul F, Haeberli W. 2012. Modeling glacier thickness distribution and bed topography over entire mountain ranges with GlabTop: Application of a

fast and robust approach. Journal of Geophysical Research 117, F03007, doi:10.1029/2011JF002313.

Linsbauer A, Frey H, Haeberli W, Machguth H, Azam MF, Allen S. 2016. Modelling glacier-bed overdeepenings and possible future lakes for the glaciers in the Himalaya–Karakoram region. Annals of Glaciology 57(71), doi:10.3189/2016AoG71A627.

NELAK. 2013. Neue Seen als Folge des Gletscherschwundes im Hochgebirge – Chancen und Risiken. Formation des nouveux lacs suite au recul des glaciers en haute montagne – chances et risques. Forschungsbericht NFP 61 (Haeberli W, Bütler M, Huggel C, Müller H, Schleiss A. (Hrsg.). Zürich, vdf Hochschulverlag AG an der ETH Zürich, 300pp.

Patton H, Swift DA, Clark CD, Livingstone SJ, Cook SJ, Hubbard A. 2015. Automated mapping of glacial overdeepenings beneath contemporary ice sheets: Approaches and potential applications. Geomorphology 232, 209-223, doi.org/10.1016/j.geomorph.2015.01.003.

Paul F, Linsbauer A. 2012. Modeling of glacier bed topography from glacier outlines, central branch lines, and a DEM. International Journal of Geographic Information Science 26, 1173–1190, doi:10.1080/13658816.2011.627859.

Portocarrero CA. 2013. Reducing the risk of dangerous lakes in the Peruvian Andes: A handbook for glacial lake management. US Agency for International Development, Washington, DC.

Ryser C, Lüthi M, Blindow N, Suckro S, Funk M, Bauder A. 2013. Cold ice in the ablation zone: Its relation to glacier hydrology and ice water content. Journal of Geophysical Research: Earth Surface 118, 693–705.

Shreve RL. 1966. Statistical law of stream numbers. Journal of Geology 74, 17-37, doi:10.1086/627137.

Suter S, Laternser M, Haeberli W, Hoelzle M, Frauenfelder R. 2001. Cold firn and ice of high-altitude glaciers in the Alps: Measurements and distribution modeling. Journal of Glaciology 47(156), 85-96.

Zemp M, Kääb A, Hoelzle M, Haeberli W. 2005. GIS-based modelling of the glacial sediment balance. Zeitschrift für Geomorphologie, Suppl.-Vol. 138, 113-129.